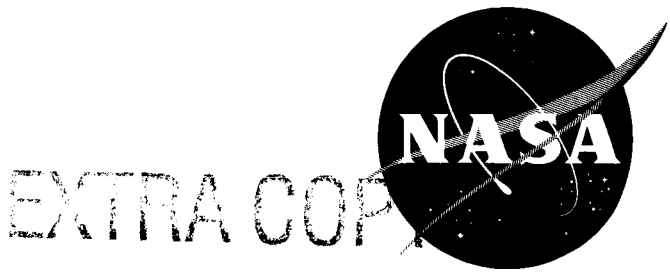

TECHNICAL NOTE

D-654

APPLICATION OF DESCRIBING-FUNCTION ANALYSIS TO THE STUDY OF AN ON-OFF REACTION-CONTROL SYSTEM

By Edgar C. Lineberry, Jr., and Edwin C. Foudriat

Langley Research Center
Langley Field, Va.

NATIONAL AERONAUTICS AND SPACE ADMINISTRATION

WASHINGTON

January 1961

NATIONAL AERONAUTICS AND SPACE ADMINISTRATION

TECHNICAL NOTE D-654

APPLICATION OF DESCRIBING-FUNCTION ANALYSIS TO THE STUDY OF AN ON-OFF REACTION-CONTROL SYSTEM

By Edgar C. Lineberry, Jr., and Edwin C. Foudriat

SUMMARY

An analytical study was made of an automatic reaction-control system for the upper stages of a missile to determine limit cycle characteristics, corresponding duty cycles, and the effects of the various system parameters on these quantities. A nonlinear servo analysis (describing function) technique was used to obtain a mathematical representation of the nonlinear components of the system.

The results obtained by this analysis are compared with the results obtained from an analog simulation including the jet reaction-control hardware. The good agreement between the results of the two studies tends to indicate the feasibility of using such an analysis technique in the early design phase of a reaction-control system, since by so doing, the parameters for good system performance can be determined quite readily.

INTRODUCTION

Reaction-control-system characteristics and requirements are usually determined by simulating the system and the dynamics of the vehicle on an analog computer. The system parameters for final design are obtained from the tests. Such techniques, while necessary, are undesirably time consuming especially for the early design stages when quick results and a clear-cut picture of the effects of various system parameters are required. Therefore, there is a need for an analytical technique which demonstrates the effects of the various system parameters and gives a good approximation to the actual results and the system modes of operation.

The analysis of a closed-loop system in which all of the system components can be represented by linear differential equations can be made by using conventional methods. However, if nonlinear components (components which display discontinuities in their operation) exist in the system, the techniques must be revised in order to handle the nonlinearities. Such is the case with the reaction-control system studied

in this paper. A theoretical analysis is made of the reaction-control system to determine the possible stable and unstable modes of operation, their corresponding duty cycles, and the effects of the various system parameters on these quantities. The describing-function technique (refs. 1 and 2) is used to obtain a mathematical representation of the nonlinear components of the system.

It is the purpose of this paper to indicate the validity of an analysis with the use of the describing-function technique and the feasibility of using such an analysis in the early design phase of a reaction-control system. Inherent in the technique is the capability of presenting clearly the effects of the system parameters upon the system operation.

SYMBOLS

A_n, B_n	Fourier series coefficients
b_j	reaction-control-thrust moment arm, ft
b_m	misalinement-thrust moment arm, ft
D	control-system dead zone, deg
F_j	reaction-control thrust, lb
F_m	misalinement thrust, lb
G	linear gain
I	moment of inertia, slug-ft^2
j	vector operator, $\sqrt{-1}$
k	ratio of valve turn-off to turn-on time
K_θ	position gain, deg/deg
$K_{\dot{\theta}}$	rate gain, $\frac{\text{deg/deg}}{\text{sec}}$
K_a	acceleration constant, $\frac{\text{deg/sec}^2}{\text{deg}}$

N	nonlinear gain
R	ratio of misalinement moment to control moment
s	Laplacian operator
t	time, sec
X	switching system input
Y	switching system output
α, β	nonlinear switching angles, radians
ζ	damping ratio
θ	pitch angle, radians
η	angular difference between on and off times, radians
τ	valve response time constant, sec
ϕ	phase angle, deg
ω	frequency, radians/sec
ω_n	undamped natural frequency, radians/sec
ω_f	limit-cycle frequency, radians/sec

Subscripts:

i	control-system input
j	reaction jet
r	control-system output
1	fundamental component
ss	steady state

A dot over a symbol designates the time derivative of the variable.

SYSTEM TO BE ANALYZED

The system being investigated controls the attitude of a missile by producing moments to overcome disturbing moments encountered by the vehicle. The restoring moments are produced by small reaction jets mounted near the base of the vehicle with thrust vectors normal to the vehicle longitudinal body axis. In this analysis the system is assumed to control the pitch attitude of the upper stages of a missile in the portion of its controlled flight where aerodynamic forces and moments can be neglected. The remaining moments consist of thrust misalinement resulting from the fixed main engine and the reaction-control moments. With the assumption that the vehicle is rigid, a single-degree-of-freedom system can be assumed, and the equation of motion becomes

$$I\ddot{\theta}_r = F_j b_j + F_m b_m \tag{1a}$$

and after burnout of the main engine is

$$I\ddot{\theta}_r = F_j b_j \tag{1b}$$

A block diagram of the control system is shown in figure 1(a), showing the nonlinear components, a reaction motor, the vehicle dynamics, and the feedback system. The feedback system includes both perfect rate and position feedback and may be obtained physically from a rate and attitude gyro combination.

The nonlinear components consist of an electronic relay with a threshold sensitivity or dead zone $\pm D$ and a two-stage electro-pneumatic valve system. The operation of the system can best be illustrated by a time sequence of operation as shown in figure 1(b). When the error signal exceeds the dead zone, as shown in the top trace, the electronic switch is actuated. A finite time τ then elapses before the pneumatic-control valve is actuated and fuel flows out of the valve. Since the valve system turn-off time may not be the same as the turn-on time, the constant k, the ratio of turn-off to turn-on time, is used so that the turn-off time is $k\tau$.

In the operation of the reaction-motor-control system, an additional time lag occurs between the time the motor is turned on and the steady-state thrust is reached, due to the buildup of gas pressure in the chamber. This lag has been approximated by a second-order system whose transfer function is

$$\frac{F_j}{Y} = \frac{(F_j)_{ss}}{\frac{s^2}{\omega_n^2} + \frac{2\zeta s}{\omega_n} + 1} \tag{2}$$

A comparison between the approximated and the actual control force is shown at the bottom of figure 1(b).

DESCRIBING-FUNCTION TECHNIQUE

For a theoretical analysis using the describing-function technique (refs. 1 and 2), the control system is divided into linear and nonlinear subsystems. Consider the closed loop system in the form shown in figure 2, with the block N representing the nonlinear components and G(s) representing the transfer function for the linear components. For the reaction-control system under consideration, the linear transfer function becomes:

$$G(s) = \frac{K_a\left(K_{\dot{\theta}}s + 1\right)}{s^2\left(\frac{s^2}{\omega_n{}^2} + \frac{2\zeta s}{\omega_n} + 1\right)} \tag{3}$$

In order for the describing-function analysis to accurately represent the operation of the system, it must be true that the linear sections of the system act as low pass filters; that is, the harmonics which may be generated in the nonlinear system are attenuated to a greater degree than the fundamental component of frequency. This technique was applied in the range where equation (3) fulfills this requirement.

For a limit cycle or steady-state oscillation to be maintained in the system, the frequency must be such that the system components produce a total phase shift of 180° when the gain in the system is unity. Using this relationship

$$NG(j\omega) = -1 \tag{4}$$

or

$$G(j\omega) = -\frac{1}{N} \tag{5}$$

The describing function is used in the analysis to represent N.

In order to determine N, an input of the form:

$$X = X_1 \cos \omega t \tag{6}$$

is imposed at the input to the nonlinear block of the system. An output is assumed in the form of a Fourier series

$$Y = A_0 + \sum_{n=1}^{\infty} (A_n \cos n\omega t + B_n \sin n\omega t) \tag{7}$$

with the coefficients as functions of the nonlinear system N. Because of the assumption that the system acts as a low pass filter, the fundamental component will be the only one considered to affect the system. Thus, the nonlinear gain N is the ratio of the fundamental component to the amplitude of the sinusoidal input, or

$$N = \frac{Y_1}{X_1} \tag{8}$$

N is determined by the describing-function method for the following cases:

Case I. Describing Function with Reaction Control (Missile Coasting)

In order to determine the gain of the nonlinear components composed of a dead zone $\pm D$ and a fuel-control valve with a time lag τ, an input of the form

$$X = X_1 \cos \omega t$$

is imposed on the system. From the previous discussion, the output is

$$Y_1 = A_0 + A_1 \cos \omega t + B_1 \sin \omega t$$

with the coefficients A_0, A_1, and B_1 to be determined.

The system operation is shown graphically in figure 3(a). The input triggers the electronic switch at $-\alpha_0$, the time τ elapses (corresponding to an angle $\omega\tau$) before the valve opens at $-\alpha_1$, and fuel begins to flow. The turn off is at α_0 and α_1', respectively. The identical operation takes place on the negative half cycle. Thus, for the positive half cycle, the angles at which the valve turn on and off are given by:

$$-\alpha_1 = -\alpha_0 + \omega\tau \tag{9}$$

and

$$\alpha_1' = \alpha_0 + k\omega\tau \tag{10}$$

The phase shift α_2 for the nonlinear system is given by:

$$\alpha_2 = \frac{\alpha_1' + (-\alpha_1)}{2} = \frac{\omega\tau}{2}(1 + k) = \phi \tag{11}$$

It is possible to shift to a new axis, α_2 shown in figure 3(b), in order to simplify the evaluation of the coefficients of the Fourier series. The input now takes the form

$$X = X_1 \cos(\omega t + \phi) \tag{12a}$$

The output takes the form

$$Y_1 = A_0 + A_1 \cos \omega t \tag{12b}$$

Since the output reaction thrusts are symmetrical and equal about the abscissa over the interval from 0 to 2π, the term A_0 is equal to zero. The A_1 term is given by

$$A_1 = \frac{2}{\pi} \int_0^{\beta_1} f(\omega t)\cos \omega t \, d(\omega t) - \frac{2}{\pi} \int_{\beta_2}^{\pi} f(\omega t)\cos \omega t \, d(\omega t) \tag{13}$$

where $f(\omega t)$, the valve output, is represented by unity. Since

$$\left.\begin{aligned} f(\omega t) &= 1 \qquad (0 \leqq \omega t \leqq \beta_1) \\ f(\omega t) &= -1 \qquad (\beta_2 \leqq \omega t \leqq \pi) \end{aligned}\right\} \tag{14}$$

and

$$\beta_2 = \pi - \beta_1 \tag{15}$$

substituting into equation (13) gives

$$A_1 = \frac{2}{\pi} \int_0^{\beta_1} \cos \omega t \, d(\omega t) - \frac{2}{\pi} \int_{\pi-\beta_1}^{\pi} \cos \omega t \, d(\omega t) \tag{16}$$

Now

$$\beta_1 = \frac{\alpha_1' - (-\alpha_1)}{2} = \alpha_0 + \frac{\omega\tau}{2}(k - 1) \tag{17}$$

and

$$D = X_1 \cos \alpha_0 \tag{18}$$

or

$$\alpha_0 = \cos^{-1} \frac{D}{X_1} \tag{19}$$

Therefore,

$$\beta_1 = \cos^{-1} \frac{D}{X_1} + \frac{\omega\tau}{2}(k - 1) \tag{20}$$

Substituting equation (20) in equation (16) and integrating gives

$$A_1 = \frac{4}{\pi} \sin\left[\cos^{-1} \frac{D}{X_1} + \frac{\omega\tau}{2}(k - 1)\right] \tag{21}$$

The describing function of the nonlinear components is given by

$$N = \frac{A_1}{X} = \frac{4}{\pi X_1} \sin\left[\cos^{-1} \frac{D}{X_1} + \frac{\omega\tau}{2}(k - 1)\right] e^{-j\phi} \tag{22}$$

where ϕ is given by equation (11).

The expression for N can now be substituted into equation (5), giving

$$- \frac{1}{\frac{4}{\pi X_1} \sin\left[\cos^{-1} \frac{D}{X_1} + \frac{\omega\tau}{2}(k - 1)\right] e^{-j\frac{\omega\tau}{2}(k+1)}} = G(j\omega) \tag{23}$$

The values of ω and $\frac{D}{X_1}$ which satisfy this relationship can be determined graphically from the intersections of the curves $G(j\omega)$ and $-\frac{1}{N}$ in a plot of gain against phase angle. Only one curve results for the linear expression $G(j\omega)$ for values of ω. For the nonlinear

expression, however, a different curve with $\frac{D}{X_1}$ as a parameter, results for each value of ω. By observing, however, that the phase angle for the nonlinear expression N varies only with ω, a value of ω can be determined where the phase angles of the two expressions $G(j\omega)$ and $-\frac{1}{N}$ are equal. Thus, at this particular value of ω, the N and the G curves represent a possible intersection point. Rearranging equation (23) and substituting the particular value of ω results in

$$\frac{1}{X_1} \sin\left[\cos^{-1}\frac{D}{X_1} + \frac{\omega\tau}{2}(k - 1)\right] = \frac{\pi}{4G} \tag{24}$$

Letting

$$C = \frac{\pi}{4G} = \text{Constant} \tag{25}$$

and

$$\eta = \frac{\omega\tau}{2}(k - 1) = \text{Constant} \tag{26}$$

gives

$$\frac{1}{X_1} \sin\left[\cos^{-1}\frac{D}{X_1} + \eta\right] = C \tag{27}$$

Applying trigonometric identities,

$$\frac{1}{X_1^2}\left[\sqrt{X_1^2 - D^2}\cos\eta + D\sin\eta\right] = C \tag{28}$$

Rearranging and solving for $\frac{D}{X_1}$ by letting

$$B = 2CD\sin\eta + \cos^2\eta \tag{29}$$

gives

$$\frac{D}{X_1} = \left[\frac{B}{2} \pm \left(\frac{B^2}{4} - C^2D^2\right)^{1/2}\right]^{1/2} \tag{30}$$

Thus two values of $\frac{D}{X_1}$ occur representing two possible oscillatory conditions.

A typical graphical diagram of the curve $N\left(\frac{D}{X_1},\omega\right)$ for one value of ω as $\frac{D}{X_1}$ varies from 0 to 1 is shown in figure 4. As shown, for a common frequency ω_f the curve for $-\frac{1}{N}$ intersects the curve for $G(j\omega)$ at two points b and c as demonstrated by equation (30).

It should be noted in figure 4 that the curves for descending and ascending gain have been separated along their abscissa for clarity. Actually the curves, because of constant phase angle, are coincident and are hereinafter plotted in that manner.

As shown in reference 1, it is necessary to determine the incremental increase or decrease in the amplitude of the output Y for an incremental increase in X_1 to determine whether the oscillatory condition corresponds to a stable or unstable limit cycle. Applying this analysis shows the first intersection for increasing X_1 to be unstable and the second intersection to be stable. Thus, the interpretation of figure 4 is that for the $\frac{D}{X_1}$ region from a to b a stable system exists in which the amplitude will die out, the region from b to c corresponds to an unstable region in which an oscillation will build up to the amplitude X_1 at c, and the region from c to d corresponds to a stable region in which the amplitude will reduce to the amplitude X_1 at c. Thus, the solutions of equation (30) correspond to the stable and unstable points, respectively.

If in equation (30)

$$C^2D^2 > \frac{B^2}{4} \tag{31}$$

a limit-cycle condition will not exist at this frequency. This relationship serves to predict the condition for which the net gain will

always be less than unity. Such a condition results in the variation of gain with phase angle for the case in which the curves for the linear and nonlinear expressions have no intersection at a common frequency. If this is the case, it is desirable to determine the gain margin (the difference between the gains of the linear and nonlinear expressions) which would be necessary to cause a limit-cycle condition. Therefore, the value of the input amplitude for minimum $\frac{1}{N}$ (or maximum nonlinear gain) must be determined. This is accomplished by differentiating $\frac{1}{N}$ with respect to X_1 and equating the resulting expression to zero, or

$$\frac{d\left(\frac{1}{N}\right)}{dX_1} = \frac{\left[\frac{4}{\pi}\sin\left(\cos^{-1}\frac{D}{X_1}+\eta\right) - \frac{4}{\pi}X_1\cos\left(\cos^{-1}\frac{D}{X_1}+\eta\right)\frac{-1}{\sqrt{1-\left(\frac{D}{X_1}\right)^2}}\left(\frac{D}{X_1^2}\right)\right]}{\frac{4}{\pi}\left[\sin\left(\cos^{-1}\frac{D}{X_1}+\eta\right)\right]^2} = 0 \tag{32}$$

Rearranging equation (32) and applying trigonometric identities,

$$X_1^2 - 2D^2 + 2D\left(X_1^2 - D^2\right)^{1/2}\tan\eta = 0 \tag{33}$$

Solving equation (33) for $\frac{D}{X_1}$ gives

$$\frac{D}{X_1} = \left(\frac{1+\sin\eta}{2}\right)^{1/2} \tag{34}$$

or the value of $\frac{D}{X_1}$ for minimum $\frac{1}{N}$. Thus, for example, for a valve with equal turn-on and turn-off time, that is, η equals zero, $\frac{D}{X_1}$ equals 0.71.

Another special condition exists, as illustrated in figure 3(a), when the valve lag time is longer than the time for the input to turn on and off the electronic switch. For this condition when

$$2\alpha_0 \leqq \omega\tau \tag{35}$$

or when substituting from equation (19)

$$\frac{D}{X_1} \leqq \cos\frac{\omega\tau}{2} \tag{36}$$

no output appears and the gain $N\left(\frac{D}{X_1},\omega\right)$ goes to zero. This represents a condition on the curve where no physical operation is possible. Thus, the maximum $\frac{D}{X_1}$ possible can be calculated as a function of the valve switching time.

The duty cycle, the time percentage of one cycle of operation that the reaction motors are on, can also be determined by the describing function. From figure 3(b),

$$\text{Duty cycle} = \frac{2\beta_1}{\pi} \tag{37}$$

Substituting equation (20) into equation (37) gives

$$\text{Duty cycle} = \frac{2\cos^{-1}\frac{D}{X_1} + \omega\tau(k-1)}{\pi} \tag{38}$$

with $\frac{D}{X_1}$ and ω determined from the stable equilibrium locus of the the curves $G(j\omega)$ and $-\frac{1}{N}$.

Case II. Describing Function for Reaction Control and Main Thrust Misalinement (Missile Thrusting)

In this analysis the gain of the secondary system composed of the nonlinear components, is determined by imposing on the system an input of the form

$$X = X_0 + X_1 \cos \omega\tau \tag{39}$$

In this case, however, the operation may not be symmetrical about the abscissa so that the output requires not only a fundamental term but also a constant term. Thus,

$$Y_1 = A_0 + A_1 \cos \omega\tau$$

The system operation is shown in figure 5 with the output now being composed of a summation of the control and misalinement moments, or

$$\left.\begin{aligned} f(t) &= F_j b_j - F_m b_m && \left(0 \leqq \omega t \leqq \alpha_1'\right) \\ f(t) &= -F_m b_m && \left(\alpha_1' \leqq \omega t \leqq \alpha_3\right) \\ f(t) &= F_j b_j - F_m b_m && \left(\alpha_3 \leqq \omega t \leqq 2\pi\right) \end{aligned}\right\} \tag{40}$$

Evaluating the angles gives

$$-\alpha_1 = -\alpha_0 + \omega\tau \tag{41}$$

$$\alpha_1' = \alpha_0 + k\omega\tau \tag{42}$$

The phase shift α_2 is given by

$$\alpha_2 = \frac{\alpha_1' + (-\alpha_1)}{2} = \frac{\omega\tau}{2}(k + 1) = \phi \tag{43}$$

As in the previous case a new axis is chosen about α_2, giving

$$A_0 = \frac{1}{\pi}\int_0^{\beta_1}\left(F_j b_j - F_m b_m\right)d(\omega t) - \frac{1}{\pi}\int_{\beta_1}^{\pi} F_m b_m \, d(\omega t)$$

$$= \frac{F_j b_j}{\pi}\beta_1 - F_m b_m \tag{44}$$

where

$$\beta_1 = \frac{\alpha_1' - (-\alpha_1)}{2} = \alpha_0 + \frac{\omega\tau}{2}(k - 1) \tag{45}$$

and

$$\alpha_0 = \cos^{-1}\frac{D - X_0}{X_1} \tag{46}$$

Substituting equations (45) and (46) into equation (44) gives

$$A_0 = \frac{F_j b_j}{\pi}\left[\cos^{-1}\frac{D - X_0}{X_1} + \frac{\omega}{2}(k - 1)\right] - F_m b_m \tag{47}$$

However, for a steady-state condition to exist A_0 must equal zero giving

$$\left[\cos^{-1}\frac{D - X_0}{X_1} + \frac{\omega\tau}{2}(k - 1)\right] = \frac{F_m b_m \pi}{F_j b_j} \tag{48}$$

which is one condition which must be fulfilled in the case of thrust misalinement.

Evaluating the fundamental or A_1 term gives

$$A_1 = \frac{2}{\pi}\int_0^{\beta_1}(F_j b_j - F_m b_m)\cos\omega t\, d(\omega t) - \frac{2}{\pi}\int_{\beta_1}^{\pi} F_m b_m \cos\omega t\, d(\omega t)$$

$$= \frac{2}{\pi} F_j b_j \sin\beta_1 \tag{49}$$

Again substituting equations (45) and (46) gives

$$A_1 = \frac{2}{\pi} F_j b_j \sin\left[\cos^{-1}\frac{D - X_0}{X_1} + \frac{\omega\tau}{2}(k - 1)\right] \tag{50}$$

Substituting equations (48) into equation (50),

$$A_1 = \frac{2F_j b_j}{\pi}\sin\left(\frac{F_m b_m \pi}{F_j b_j}\right) \tag{51}$$

Rearranging equation (51) and letting

$$\frac{F_m b_m \pi}{F_j b_j} = R \tag{52}$$

gives

$$A_1 = 2F_m b_m \frac{\sin [R]}{R} \tag{53}$$

The nonlinear expression is thus

$$N = \frac{A_1}{X_1} e^{-j\phi} = \frac{2F_m b_m}{X_1} \frac{\sin [R]}{R} e^{-j\frac{\omega T}{2}(k+1)} \tag{54}$$

Substituting equation (54) into equation (5) yields

$$- \frac{1}{\frac{2F_m b_m}{X_1} \frac{\sin [R]}{R} e^{-j\frac{\omega T}{2}(k+1)}} = G(j\omega) \tag{55}$$

A graphical solution is necessary to determine the value of ω and X_1 which satisfy the relationship. Again noting that the phase angle of nonlinear expression varies only with ω a value of ω can be determined for which the phase angles of the two expressions are equal. Substituting the value of linear gain which corresponds to the particular value of ω into equation (55) yields

$$\frac{1}{\frac{2F_m b_m}{X_1} \frac{\sin [R]}{R}} = G$$

or

$$X_1 = \frac{2F_m b_m G \sin [R]}{R} \tag{56}$$

Thus, only one value of X_1 results for a limit-cycle condition. Equation (54) shows that the nonlinear gain varies inversely with X_1, and disturbances in the input amplitude would cause oscillations either to build up or to decay back to the value given by equation (56). Thus, equation (56) represents a stable equilibrium condition.

The steady-state error X_0 can also be determined for the equilibrium condition. By equation (48)

$$\cos^{-1}\frac{D - X_0}{X_1} + \frac{\omega\tau}{2}(k - 1) = \frac{\pi F_m b_m}{F_j b_j}$$

or

$$X_0 = -X_1 \cos\left[\frac{\pi F_m b_m}{F_j b_j}\frac{\omega\tau}{2}(1 - k)\right] + D \tag{57}$$

The duty cycle can be expressed by

$$\text{Duty cycle} = \frac{\beta_1}{\pi} \tag{58}$$

or, by equation (45) and equation (46),

$$\text{Duty cycle} = \frac{\cos^{-1}\frac{D - X_0}{X_1} + \frac{\omega\tau}{2}(k - 1)}{\pi} \tag{59}$$

Substituting equation (48) yields

$$\text{Duty cycle} = \frac{F_m b_m}{F_j b_j} \tag{60}$$

Thus the duty cycle is simply the ratio of the misalinement to the reaction-control moment.

This study does not consider another mode of operation which might exist for a condition of smaller main-thrust misalinement. In looking again at figure 5, if the misalinement thrust is sufficiently small compared with the control thrust, the error signal will cross the dead zone $-D$ in the negative half cycle and cause a control-thrust pulse. Such a condition is amenable to the describing-function analysis in the same manner as the two cases previously discussed. However, it was not considered to be as critical for design purposes as the cases investigated.

RESULTS AND DISCUSSION

The results obtained by applying the describing-function technique are compared with the results obtained in a simulation of an actual vehicle reaction-control system. In the simulation study the actual hardware, including reaction motors, was used in conjunction with an analog computer which simulated the dynamics of the vehicle.

The system parameters used in the analytical study are the best estimates of the hardware characteristics from the simulation study in order that a comparison of the results of the two studies might be made. These parameters are presented in table I. In the simulation study, exponential functions were used to approximate the peak, nominal, and decaying thrust of the main engine. For the analytical study, however, only the nominal thrust value was used with an engine burning time determined by the value of total impulse used in the simulation study.

Missile Coasting Phase

By using the analytical techniques developed in the previous sections and the hardware parameters shown in table I, an analysis of the coasting phase of flight has been made. Figures 6 and 7 show plots of equation (23) for lag times of "slow" and "fast" valves, respectively, and a nominal thrust level of 486 pounds.

Figure 6 shows gain plotted against phase angle for various values of frequency and input amplitude for the nonlinear expression $\left(-\frac{1}{N}\right)$. As noted previously, a single curve can be used to describe $G(j\omega)$ with frequency as a parameter. However, separate curves are required for each value of ω for the nonlinear expression $-\frac{1}{N}(j\omega)$. Each of these curves is vertical and extends from a gain of infinity to a minimum at approximately 27db and then back to a maximum as $\frac{D}{X_1}$ varies from 0 to 1. Since the range of general interest will be between $\frac{D}{X_1}$ of 0.1 to 0.9, only this range has been shown on most of the curves. Attention should again be called to figure 4 to note that this line is double valued. As can be seen in figures 6 and 7, increasing frequencies cause the phase of $\frac{D}{X_1}$ to vary from -178° at $\omega = 0.25$ to -69° at $\omega = 15$.

In figure 6 an intersection of the curves for $G(j\omega)$ and $-\frac{1}{N}$ occurs for a common frequency of 8.14 radians/sec. This corresponds

to the frequency where limit-cycle oscillations can take place. At this point $\frac{D}{X_1}$ values of 0.565 and 0.775 occur. As previously discussed with figure 4, there are two possible modes of stable operation; the input amplitude will die out if the system is operating at a $\frac{D}{X_1}$ value greater than 0.775, and a limit cycle at the amplitude $X_1 = \frac{D}{0.565}$ will occur for a $\frac{D}{X_1}$ value less than 0.775. Thus a shock-excited limit cycle is possible, and indeed in the hardware test one did exist at a measured frequency of 6.8 radians/sec. The duty cycle predicted from the analysis using equation (38) is 58 percent which compares favorably with the 48-percent duty cycle obtained from the actual tests.

It could be reasoned that with proper adjustment a $\frac{D}{X_1}$ value greater than 0.775 could be maintained, and thus no limit cycle would exist. Theoretically this may be possible, but in the analysis it was shown that a maximum value of $\frac{D}{X_1}$ also exists. This has also been plotted as the dotted line on figure 6. Thus, the only permissible range, as illustrated by equation (30), in which a limit-cycle condition will not exist is from $\frac{D}{X_1}$ of 0.844 to 0.775. It can be argued intuitively that this is not a sufficient gain range (approximately 1db) for operation without the existence of a limit cycle and that the impulse thrust from a reaction motor firing will have sufficient frequency content at the resonant frequency to cause the system to be shock excited into a limit-cycle oscillation.

Figure 7 shows the same system operation with fast valves. Here no intersection of the $G(j\omega)$ and $-\frac{1}{N}$ curves takes place for a common frequency under the assumed conditions. Therefore, no limit-cycle frequency will exist at this point. This was found to be true in the hardware tests. It should be noted that this system has a 6db gain margin before limit-cycle oscillations at 17.1 radians/sec would take place.

Only one value of rate gain, $K_{\dot{\theta}} = 0.4$, was used in the hardware tests. A survey of the feedback stabilization gains was made analytically in order to determine the best possible gain, $K_{\dot{\theta}}$, for the slow values and a nominal thrust level of 486 pounds. The results are shown

in figure 8 where the grid of values plotted shows the $G(j\omega)$ loci for frequencies from 3 to 10 radians/sec and values of $K_{\dot{\theta}}$ from 0.1 to 1.0 deg/deg/sec. Plotted also are the $-\frac{1}{N}$ curves for the same range of frequencies and the maximum value of the nonlinear gain, N_{max}, $\left(\text{corresponding to minimum } \frac{1}{N}\right)$ obtained by using equation (34). The dashed curve shows the loci of the intersections of the curves $G(j\omega)$ and $-\frac{1}{N}$ or the limit-cycle conditions. Under the conditions assumed the best gain range is for $0.22 < K_{\dot{\theta}} < 0.37$ since for these conditions the curves do not intersect since the points are below N_{max} line. However, since the gain margin is on the order of 1db it is expected that the system operation would be critically dependent upon hardware variations.

If the higher thrust level of 586 pounds was used, a limit-cycle condition would exist for all values of rate gain. However, it would still be desirable to specify those rate gains which give minimum duty cycle since they correspond directly to minimum fuel expenditure. This has been determined by use of equations (30) and (38) and is plotted in figure 9. For these conditions gains of $K_{\dot{\theta}} > 0.28$ give the better conditions for minimum duty cycle.

Missile Burning Phase

An analysis of the operating conditions for the missile during its burning phase has been made by using the previously developed techniques and the results compared with the actual analog tests. A graphical determination of the limit-cycle conditions using equation (55) for the fast and slow valves is shown in figures 10 and 11, respectively, at a point in time 16 seconds after the ignition of the main engine.

These figures show that an oscillatory condition will always exist at the frequency of intersection. By using equation (60) and the values from figure 10, the duty-cycle and limit-cycle conditions plotted against thrust misalinement are shown for the fast valves in figure 12. Also plotted in figure 12 are the data from the analog tests. A similar set of curves are shown in figure 13 for the operation of the slow valves.

The figures show a reasonable and conservative estimate for the duty cycle. The calculated values of duty cycle are greater than the corresponding test values. This discrepancy can be accounted for, however, by the fact that nominal thrust levels were assumed for the calculated values. During high-frequency operation of the rocket motors,

however, the transient thrust period becomes predominant, and the average thrust over the time interval of operation is greater than the nominal value. The two results will give identical values in the determination of fuel consumption during a specified time interval if average thrust values are used in the analytical equation.

However, for the limit-cycle condition, agreement is not as good because the analytical results predict that the frequency of limit cycle does not change with thrust misalinement while the test data show a definite increase with increasing misalinement. One factor which has been neglected in the approximation and which might account for this discrepancy is the effect of the higher harmonics on the input to the system. Since the amount of harmonic content present is altered for different values of R, this could, in turn, alter the limit-cycle frequency. The method for analyzing the effect of higher harmonics is shown in reference 2, but since this method is long and tedious, no attempt has been made to apply it to these results. It is true, however, that the results do afford a good prediction to the average frequency of the limit cycle, as is shown in figure 14.

The describing function by using equation (57) can also be used to predict the steady-state error about which the system oscillates. Figure 15 shows that very good agreement exists between the analytical and test results.

Reaction-Control Fuel Consumption

The values of duty cycle previously determined were used to compute the reaction-control fuel consumption for a 30.85-second period of main rocket motor burning followed by a 5-second coast period. The following assumptions were used in making the calculations:

(1) The reaction motor burns for 2 seconds during the first 5 seconds to overcome initial transients.

(2) A limit-cycle condition exists for the remainder of the main motor burning period.

(3) A limit-cycle condition exists for the entire 5-second coast period when the slow valves are employed.

(4) When fast valves are used, an arbitrary duty cycle of 10 percent is assumed during the coast period.

By using these assumptions, the fuel consumed over the time interval was determined by dividing the total impulse by the specific impulse

of the fuel. The analytical results are compared with the fuel-consumption test results obtained by determining the actual fuel weight differential for the test run. The comparison is shown in figure 16. As indicated by the figure, excellent agreement exists between the results of the two studies.

CONCLUDING REMARKS

The analysis, discussion, and comparison with actual hardware tests have illustrated that by use of the describing-function technique, it is possible to predict by analytical techniques some of the important factors involved with the design of an on-off reaction-control system. The following conclusions can be stated:

1. The technique is applicable to the condition of main engine thrusting and coasting phases of flight.

2. The limit-cycle frequency can be estimated for both phases.

3. The duty cycles can be obtained for both phases. From the duty cycle it is possible to estimate the quantity of fuel used.

4. The parameters which affect the existence of a limit-cycle frequency for the coast phase can be studied. The effect of feedback, thrust level, dead band, and valve lag can all be taken into account in the design analysis.

5. The results of the analytical study show good correlation with results obtained in an analog simulation including reaction-control hardware.

Langley Research Center,
National Aeronautics and Space Administration,
Langley Field, Va., October 31, 1960.

REFERENCES

1. Truxal, John C.: Automatic Feedback Control System Synthesis. McGraw-Hill Book Co., Inc., 1955, pp. 559-612.

2. Cosgriff, Robert Lien: Nonlinear Control Systems. McGraw-Hill Book Co., Inc., 1958, pp. 170-221.

TABLE I.- SYSTEM PARAMETERS

Reaction motor characteristics (dynamic response of eq. (2)):	
Nominal thrust level, $(F_j)_{ss}$, lb	486 and 586
Damping, ζ	0.6
Undamped natural frequency, ω_n, radians/sec	45
Valve response:	
Slow valves -	
Amount of time to turn on, sec	0.14
Amount of time to turn off, sec	0.12
Fast valves -	
Amount of time to turn on, sec	0.06
Amount of time to turn off, sec	0.05
System dead zone, radian	± 0.014
Main-thrust-misalinement angle, deg	0.1, 0.1769, and 0.25
Main-engine thrust, lb	63,000
Burning time, sec	30.85
Vehicle coast time, sec	5
Pitching moment of inertia ($0 \leq t \leq 30$), I, slug-ft^2	$32{,}700 - 265t - 5.6t^2$
Reaction-control-thrust moment arm ($0 \leq t \leq 30$), b_j, ft	$14 + 0.0064t^2$
Misalinement-thrust moment arm ($0 \leq t \leq 30$), b_m, ft	$15.6 + 0.0064t^2$
Position gain, K_θ, deg/deg	1
Rate gain, $K_{\dot{\theta}}$, $\frac{\text{deg/deg}}{\text{sec}}$	0.4
Specific impulse of hydrogen peroxide, $\frac{\text{lb-sec}}{\text{lb}}$	132

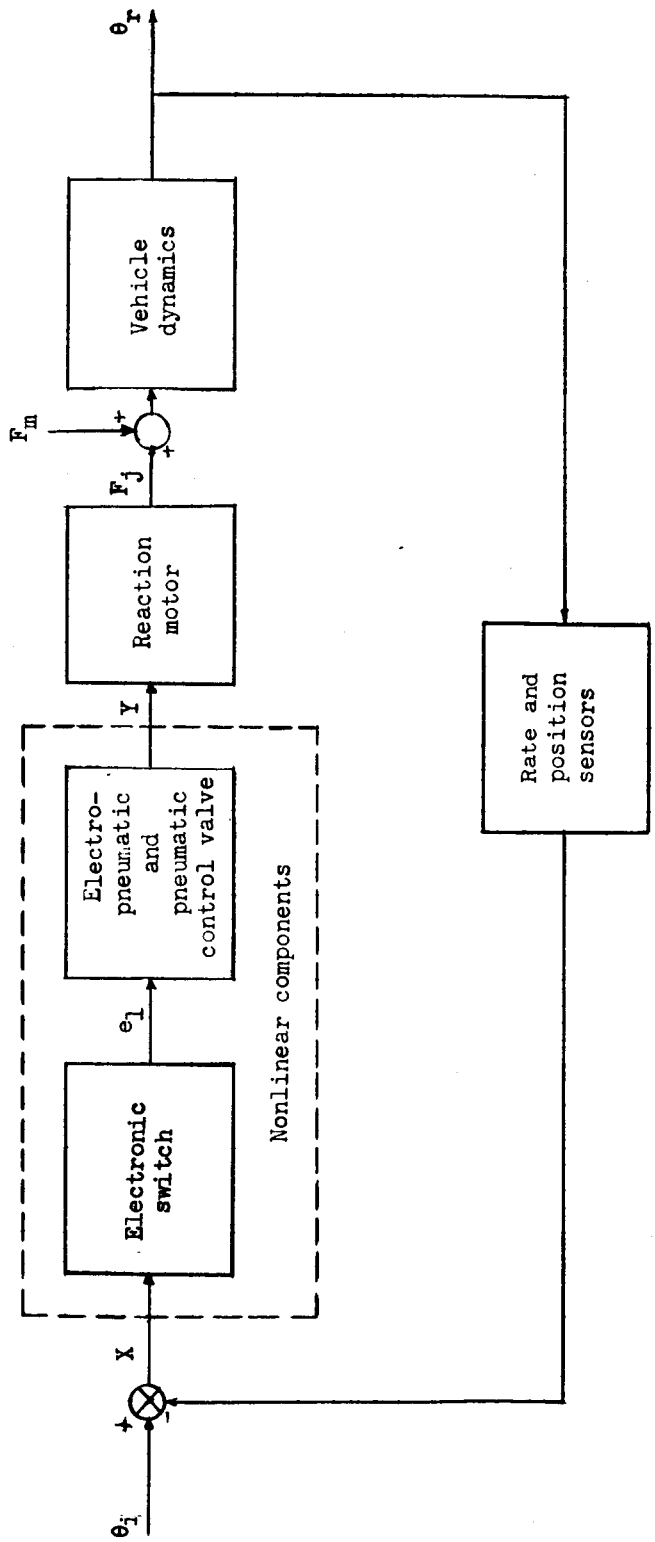

(a) Block diagram of system.

Figure 1.- Reaction-control system.

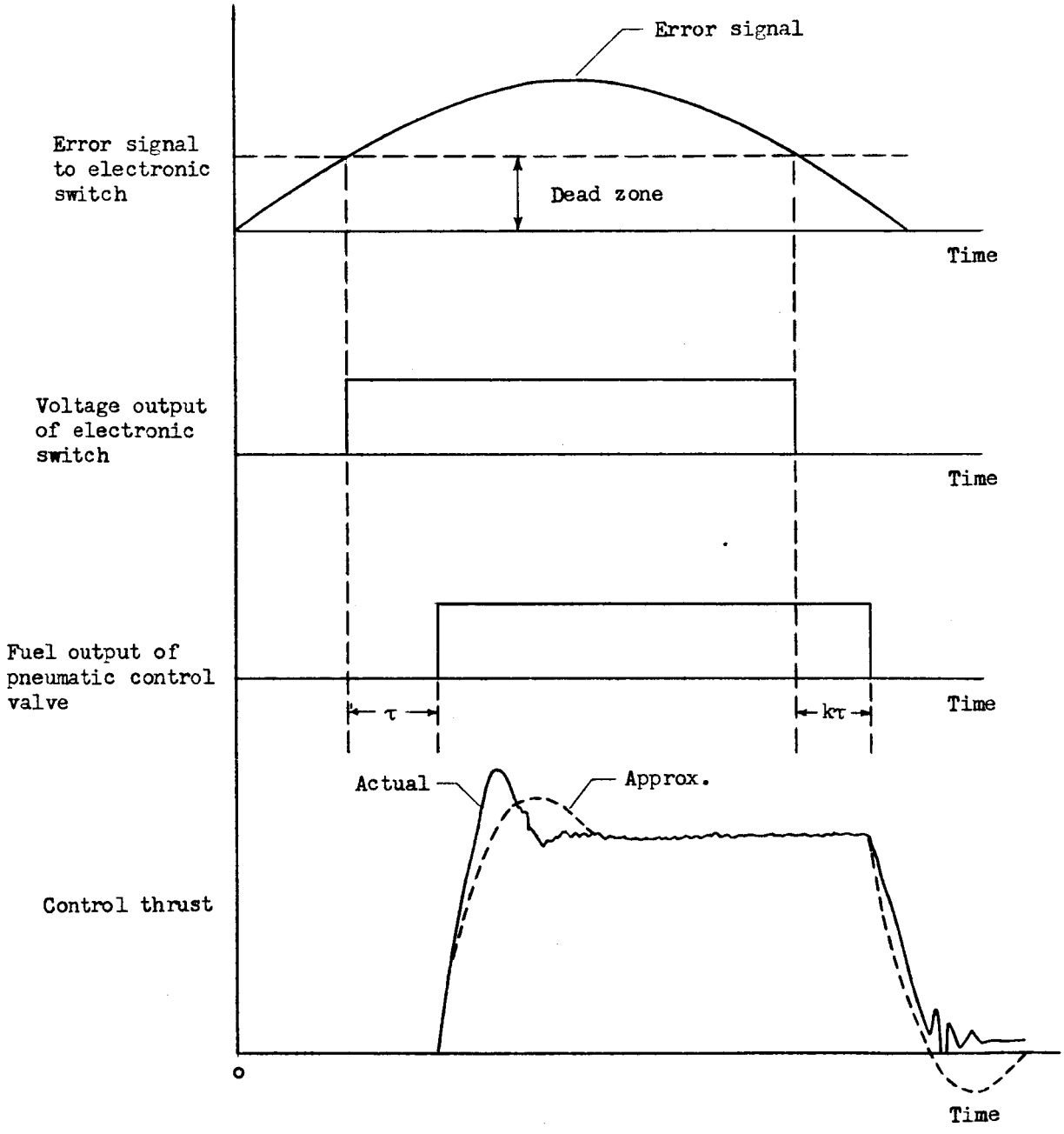

(b) Sequential operation of system.

Figure 1.- Concluded.

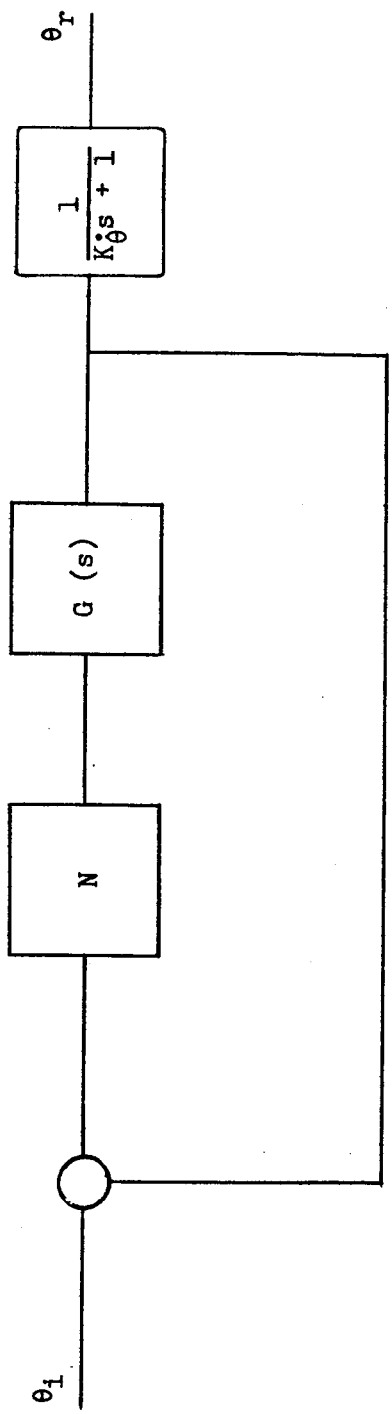

Figure 2.- Equivalent block diagram showing linear and nonlinear subsystems.

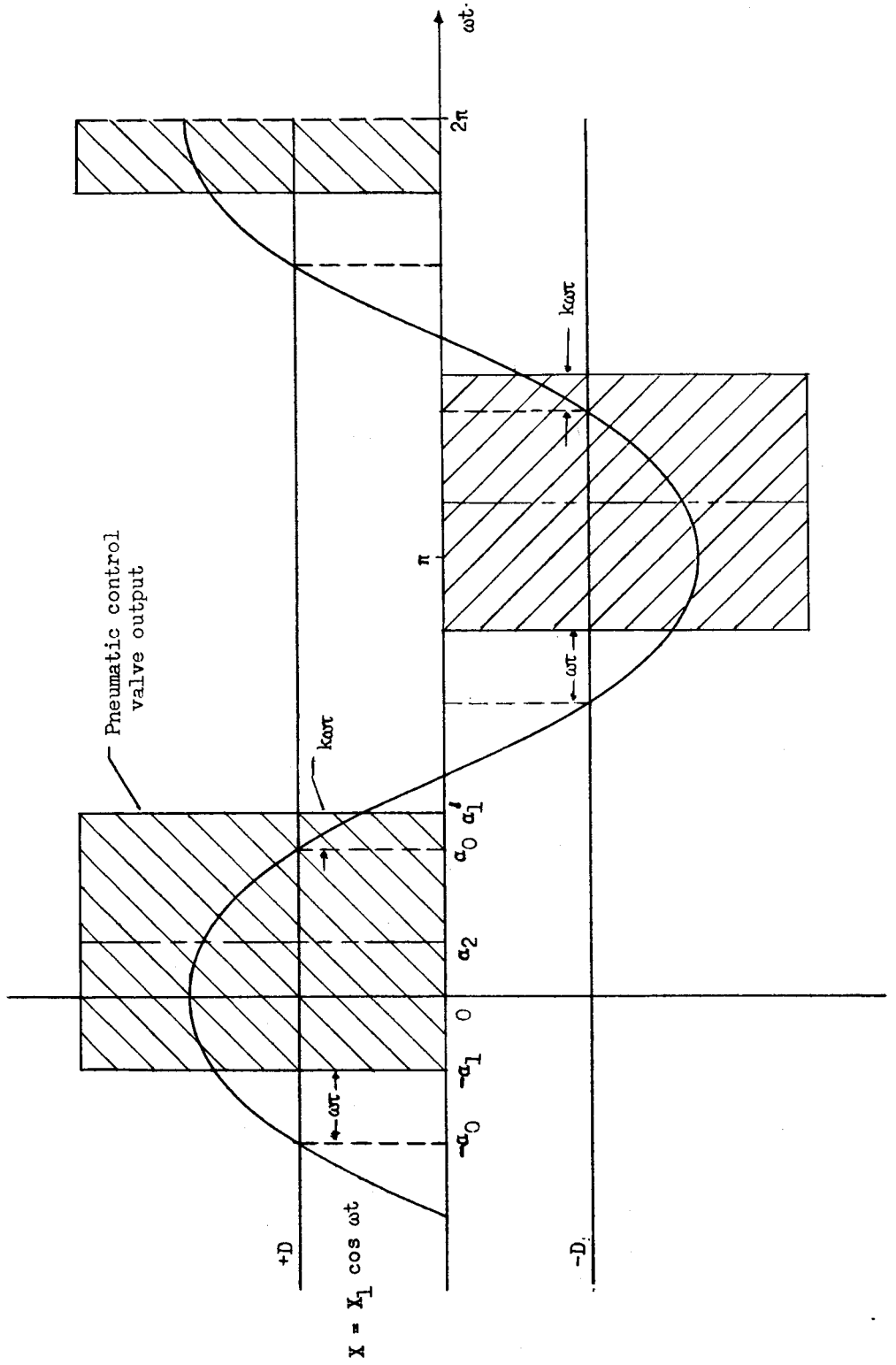

(a) Asymmetrical output along time axis.

Figure 3.- Operation of nonlinear system (missile coasting).

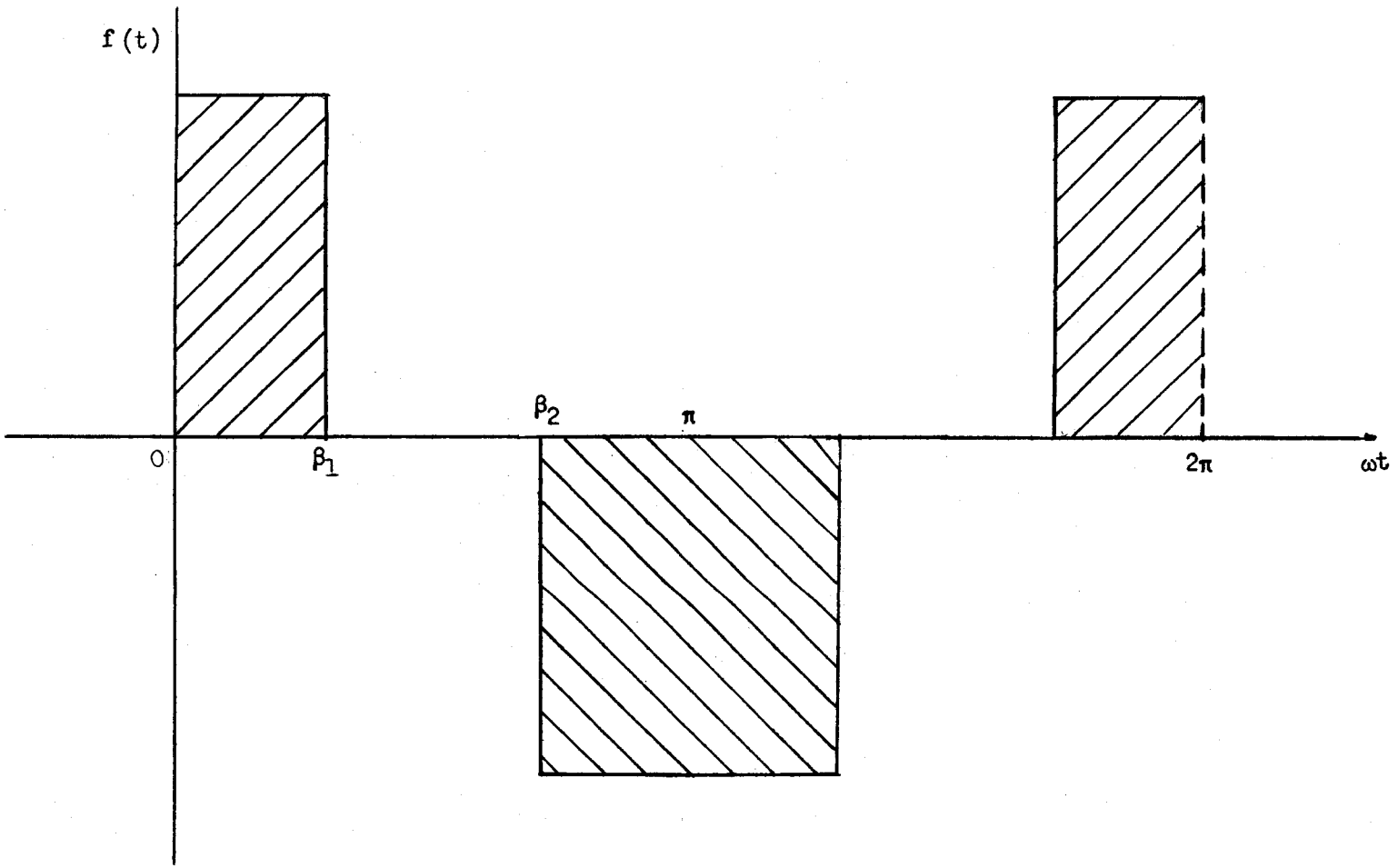

(b) Symmetrical output along time axis.

Figure 3.- Concluded.

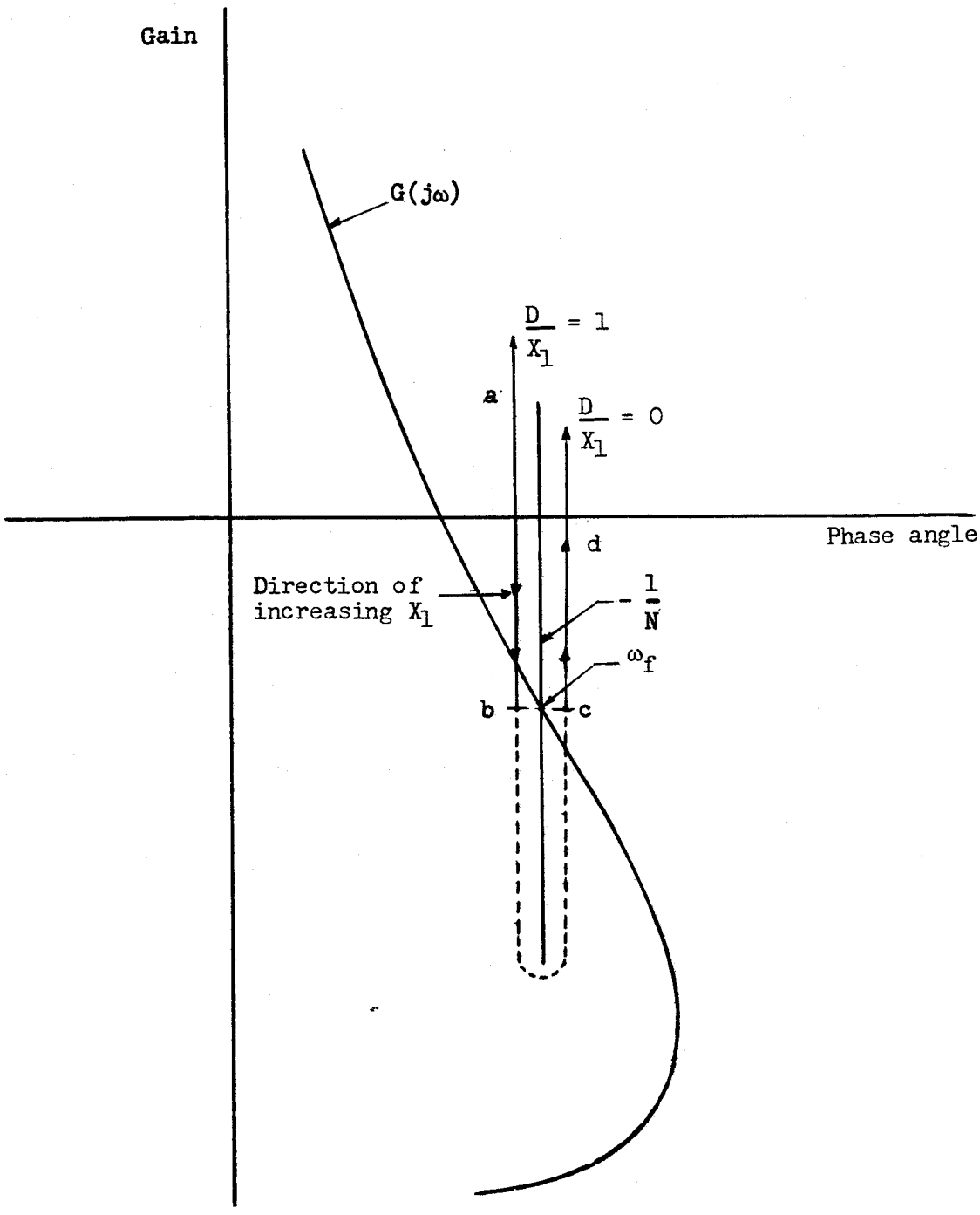

Figure 4.- Limit-cycle stability analysis.

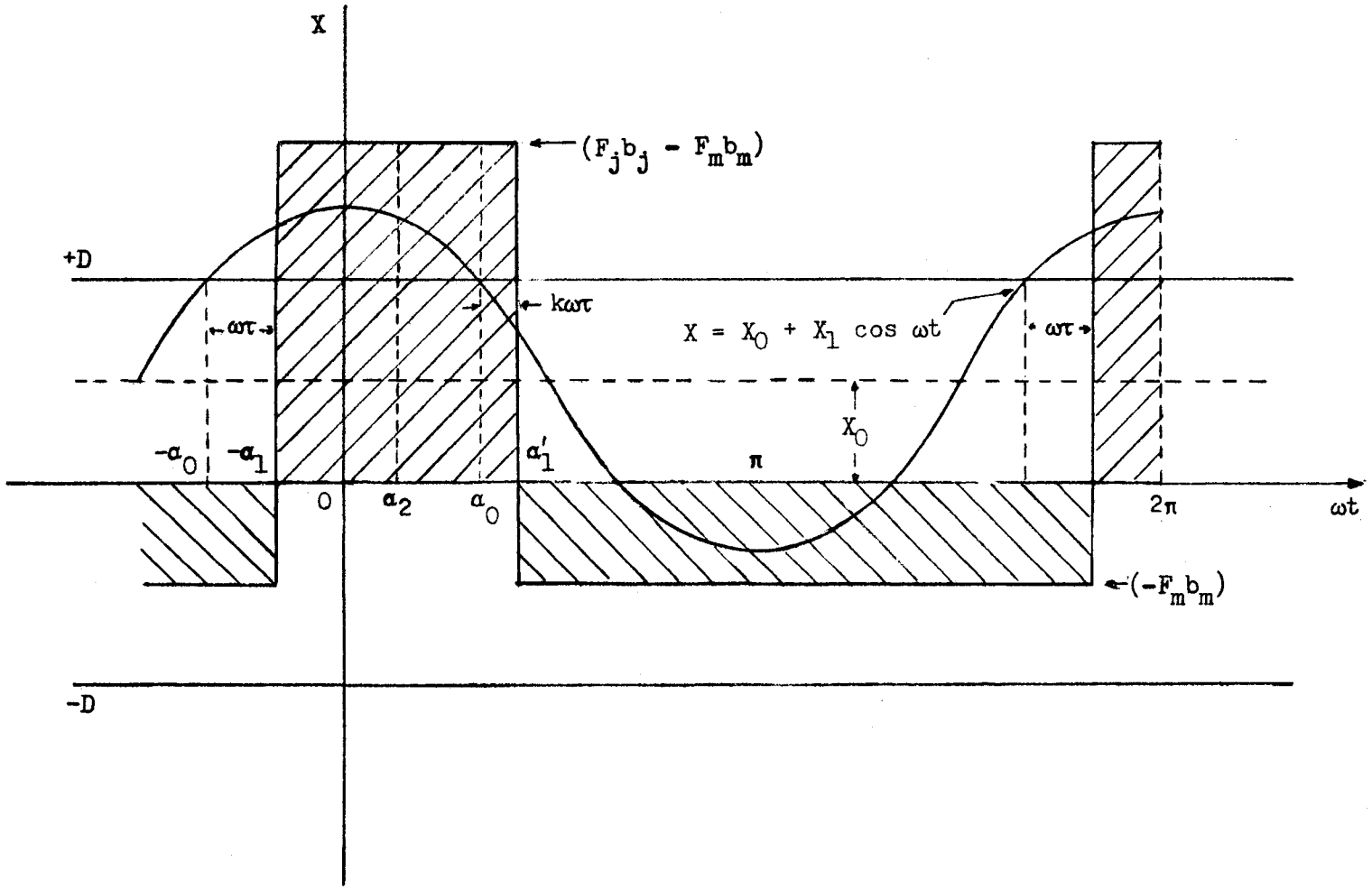

Figure 5.- Operation of nonlinear system (missile thrusting with main-thrust misalinement).

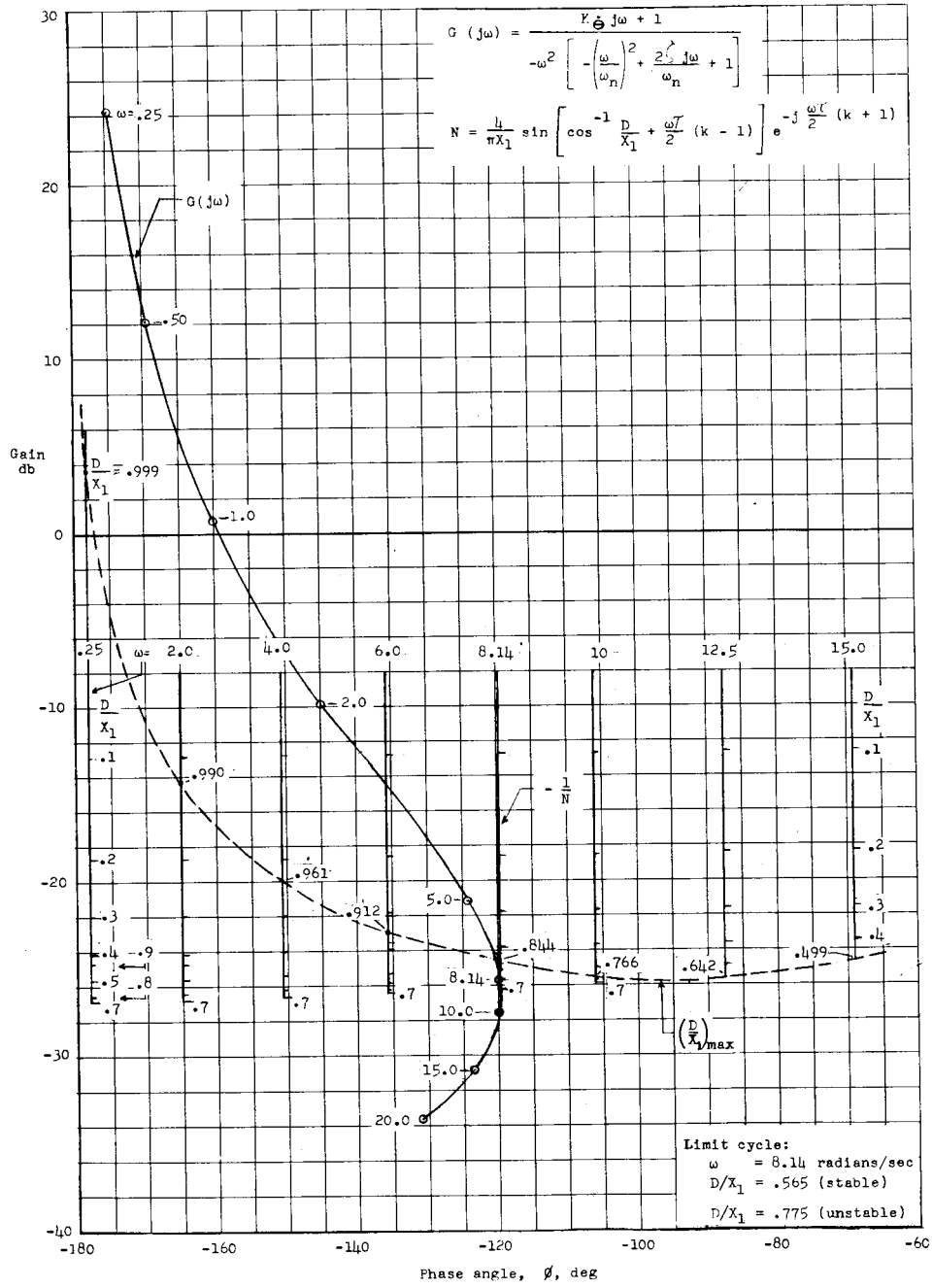

Figure 6.- Variation of gain with phase angle for limit-cycle determination during period of missile coasting. $K_{\dot\theta} = 0.4 \frac{\text{deg/deg}}{\text{sec}}$; $\tau = 0.14$ sec; $k = 0.85$; $F_j = 486$ lb; $\zeta = 0.6$; $\omega_n = 45$ radians/sec.

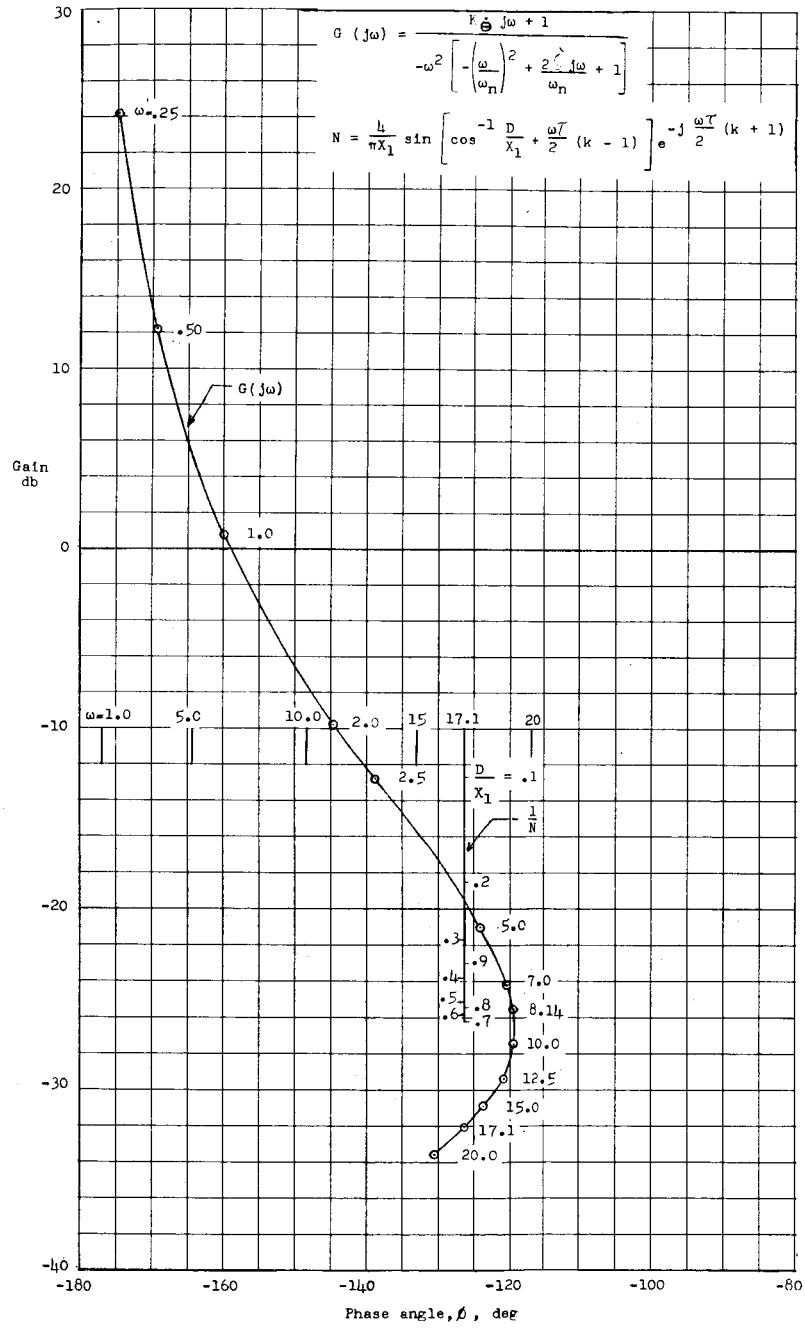

Figure 7.- Variation of gain with phase angle for limit-cycle determination during period of missile coasting. $K_{\dot{\theta}} = 0.4 \frac{\text{deg/deg}}{\text{sec}}$; $\tau = 0.06$ sec; $k = 0.83$; $F_j = 486$ lb; $\zeta = 0.6$; $\omega_n = 45$ radians/sec.

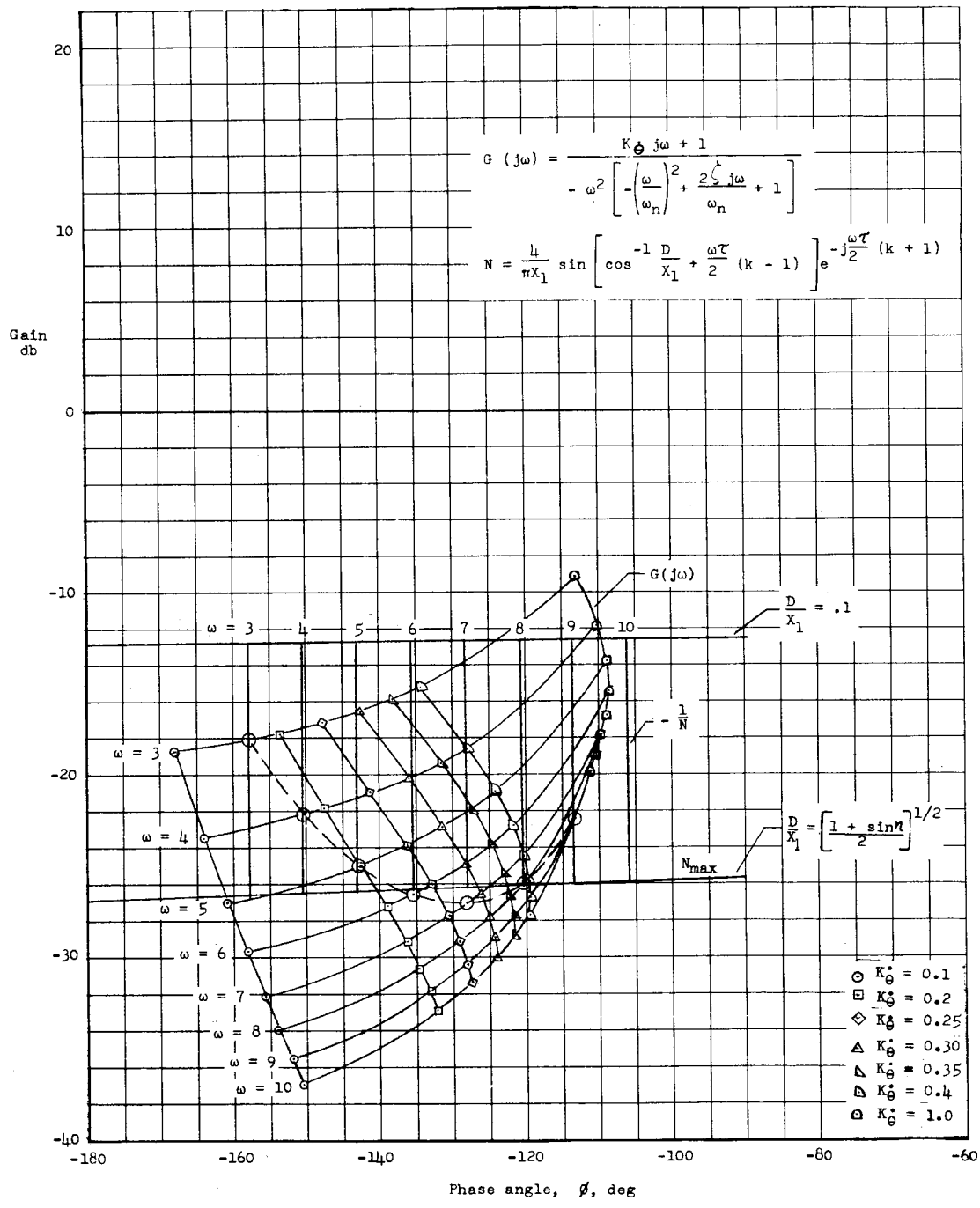

Figure 8.- Variation of limit-cycle frequency with rate gain during period of missile coasting. $K_{\dot\theta}^* = 0.4 \frac{\text{deg/deg}}{\text{sec}}$; $\tau = 0.14$ sec; $k = 0.85$; $F_j = 486$ lb; $\zeta = 0.6$; $\omega_n = 45$ radians/sec.

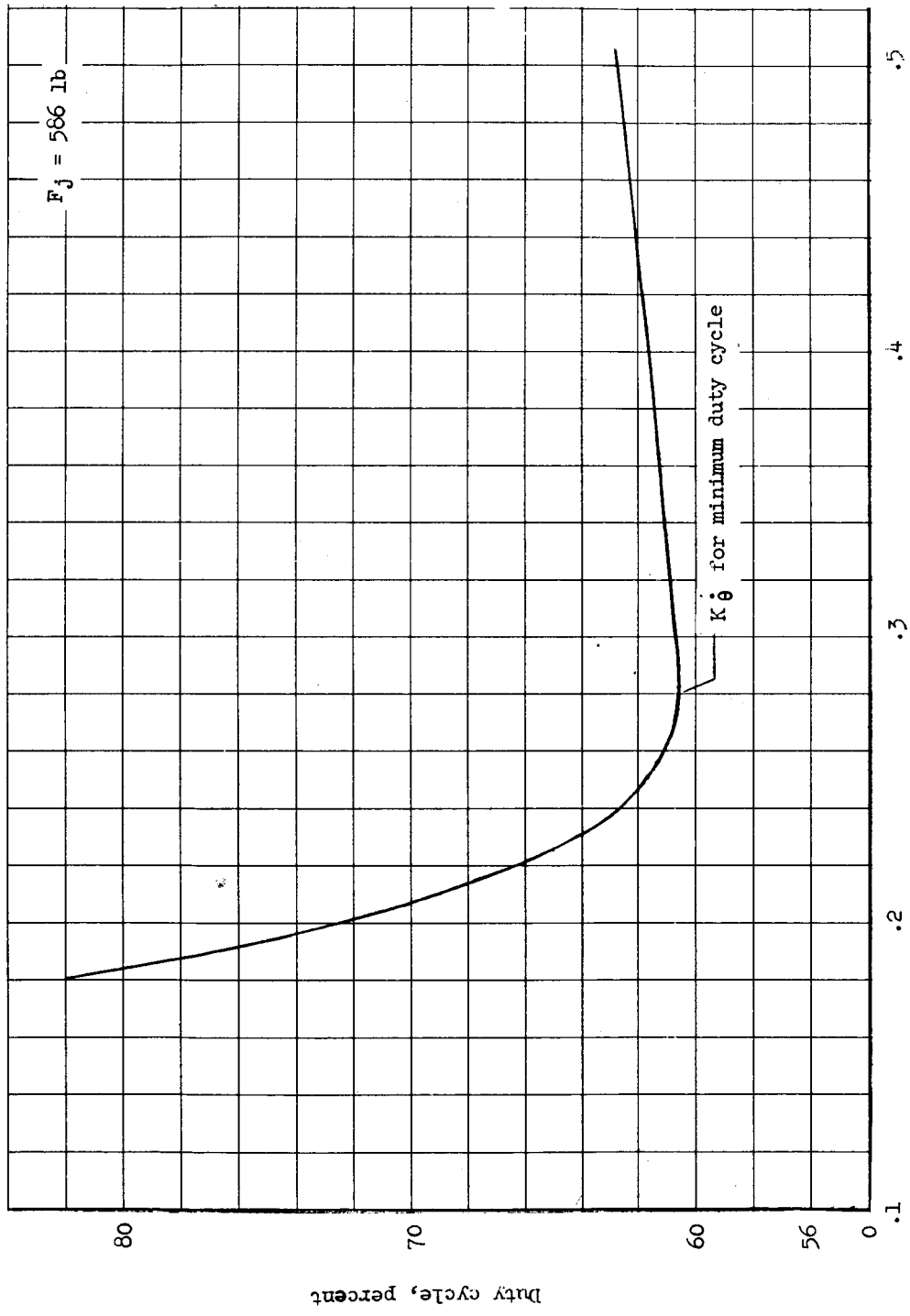

Figure 9.- Variation of duty cycle with rate gain.

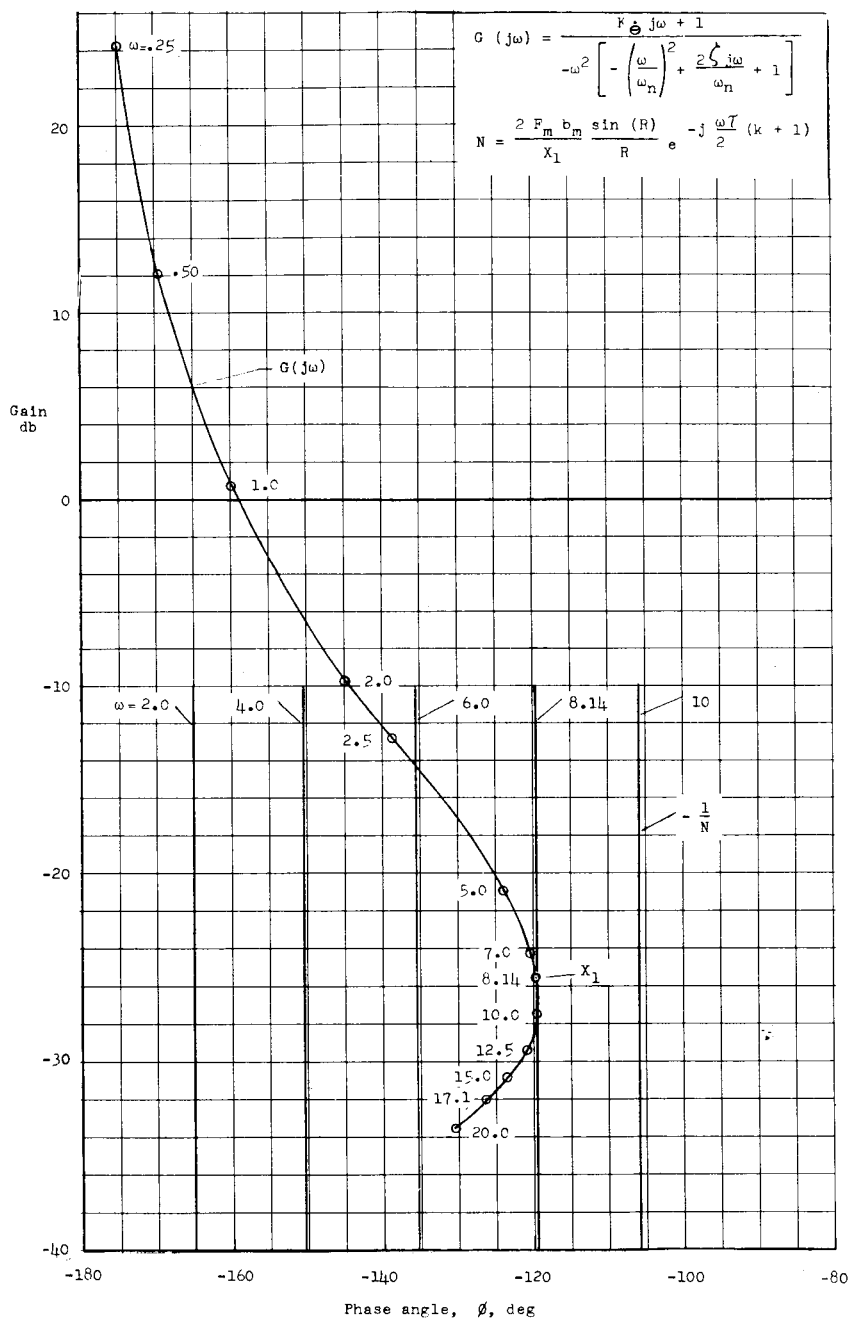

Figure 10.- Variation of gain with phase angle for limit-cycle determination during period of main-engine burning (t = 16 sec).

$K_{\dot{\theta}} = 0.4 \frac{\text{deg/deg}}{\text{sec}}$; $\tau = 0.14$ sec; $k = 0.85$; $F_j = 486$ lb; $\zeta = 0.6$; $\omega_n = 45$ radians/sec.

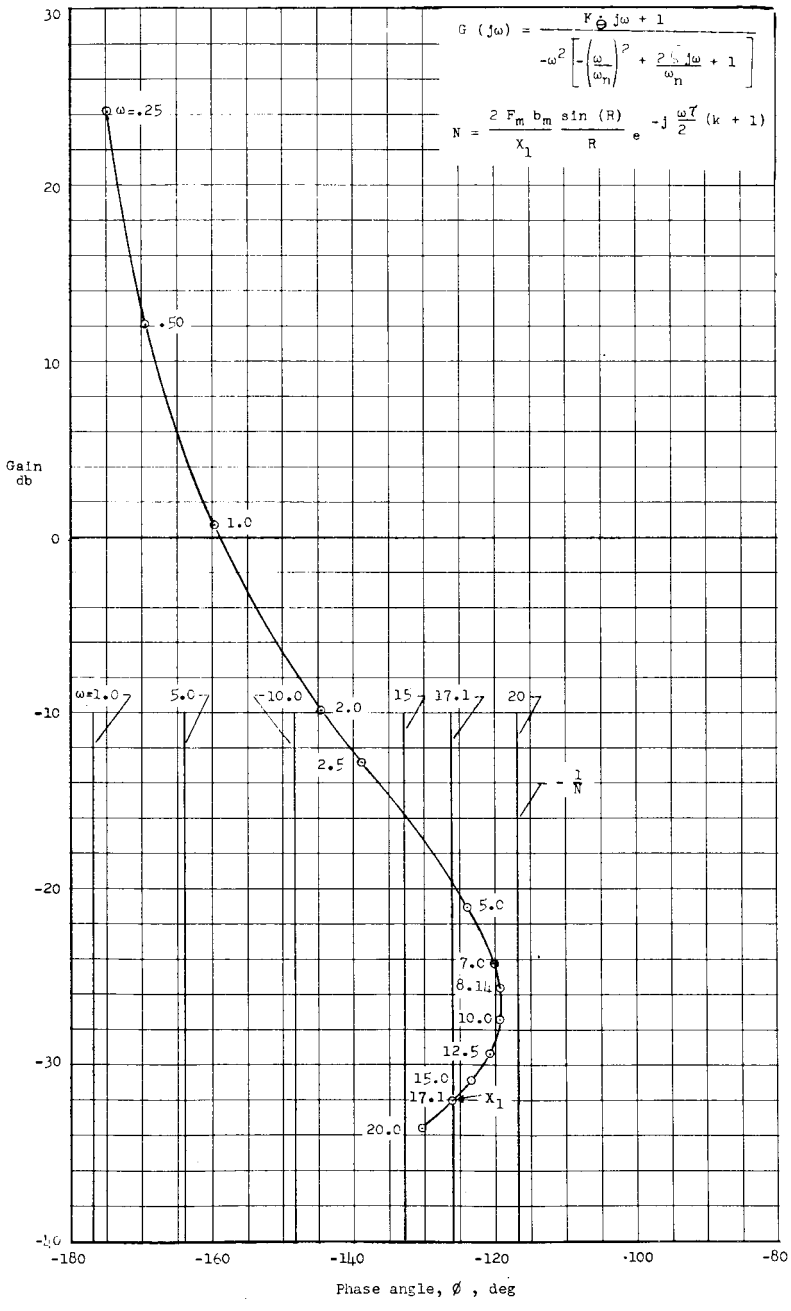

Figure 11.- Variation of gain with phase angle of limit-cycle determination during period of main-engine burning (t = 16 sec).
$K_{\dot{\theta}} = 0.4 \frac{\text{deg/deg}}{\text{sec}}$; $\tau = 0.06$ sec; $k = 0.83$; $F_j = 486$ lb; $\zeta = 0.6$; $\omega_n = 45$ radians/sec.

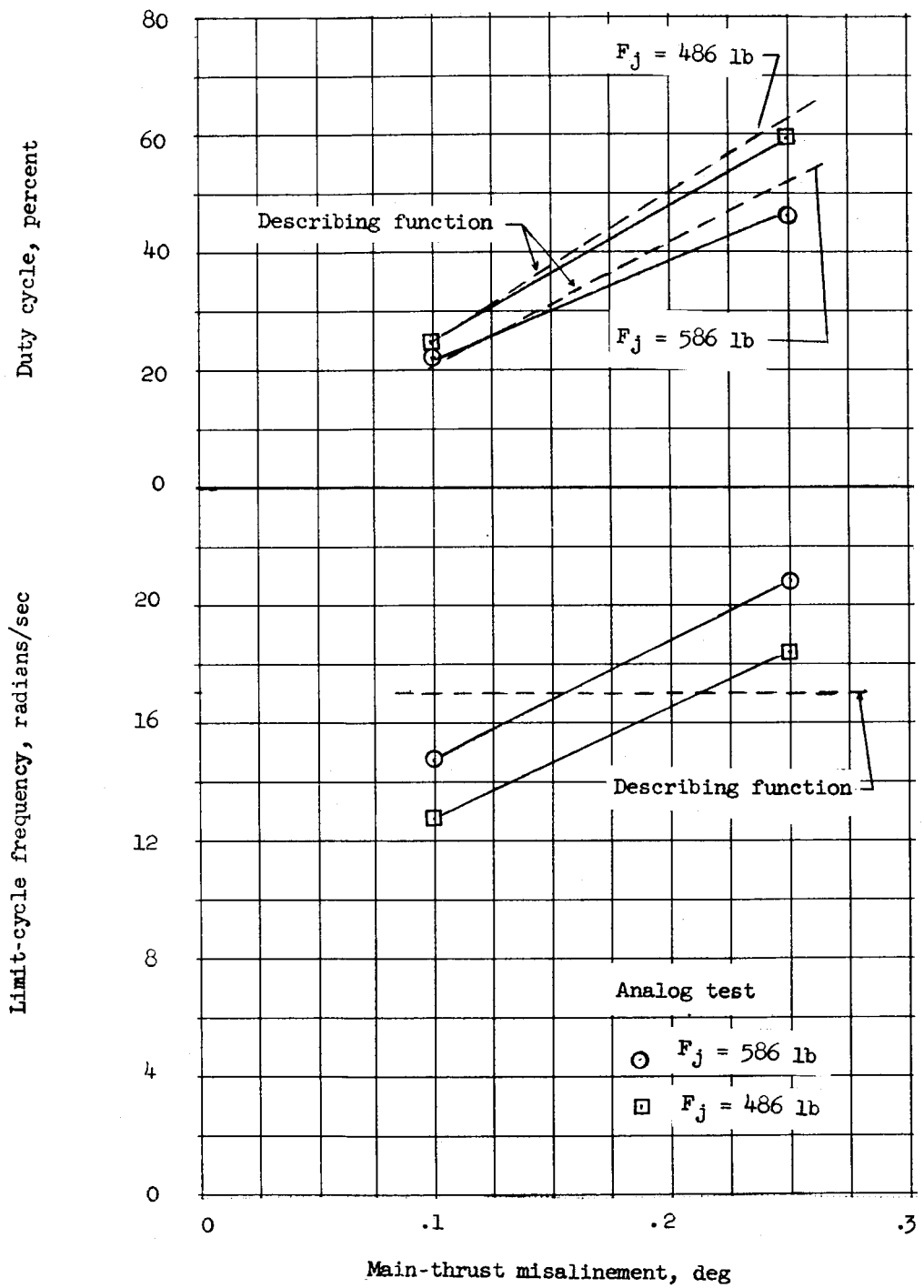

Figure 12.- Variation of limit-cycle frequency and duty cycle with main-thrust misalinement. (τ = 0.06 sec.)

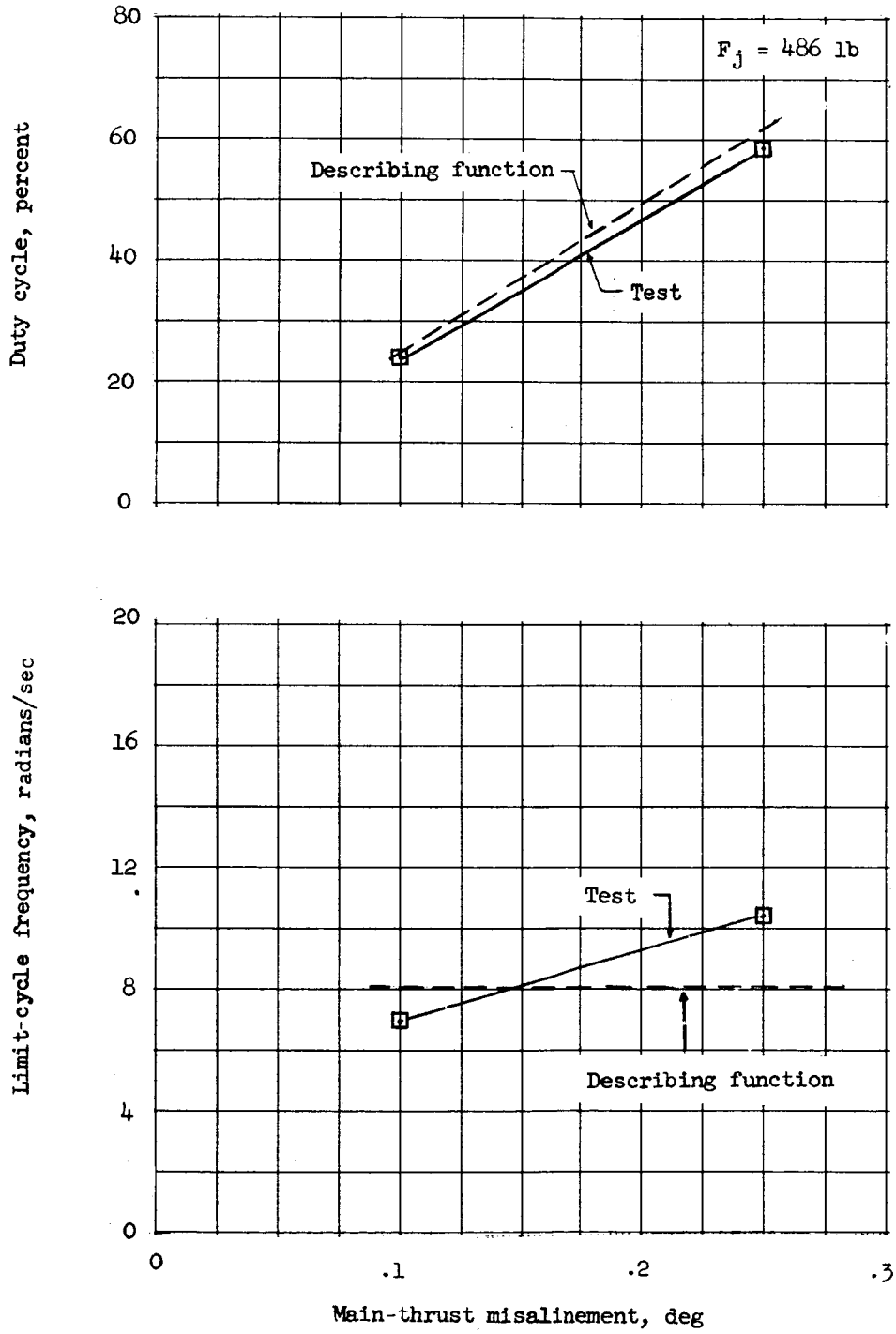

Figure 13.- Variation of limit-cycle frequency and duty cycle with main-thrust misalinement. (τ = 0.14 sec.)

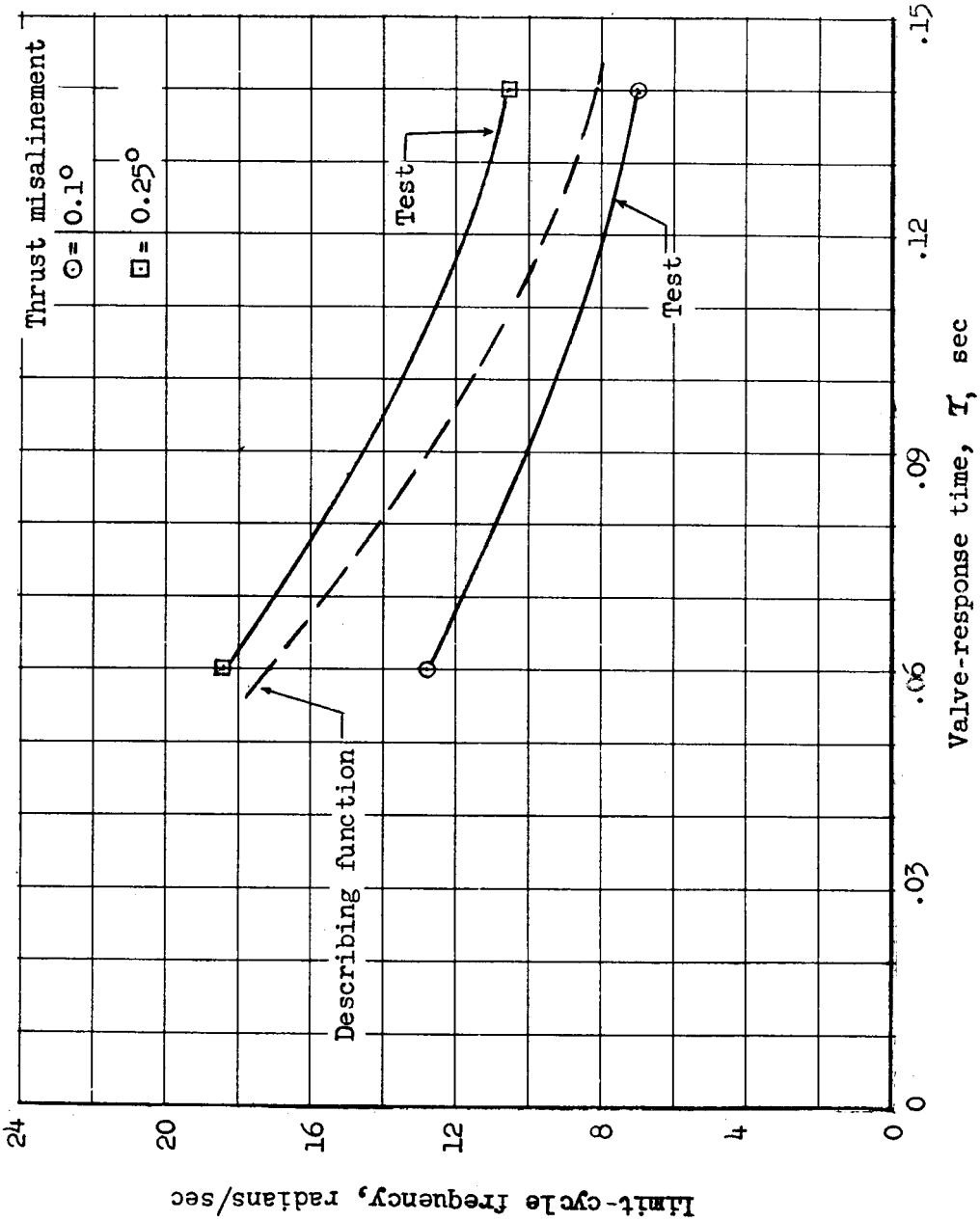

Figure 14.- Variation of limit-cycle frequency with valve-response time.

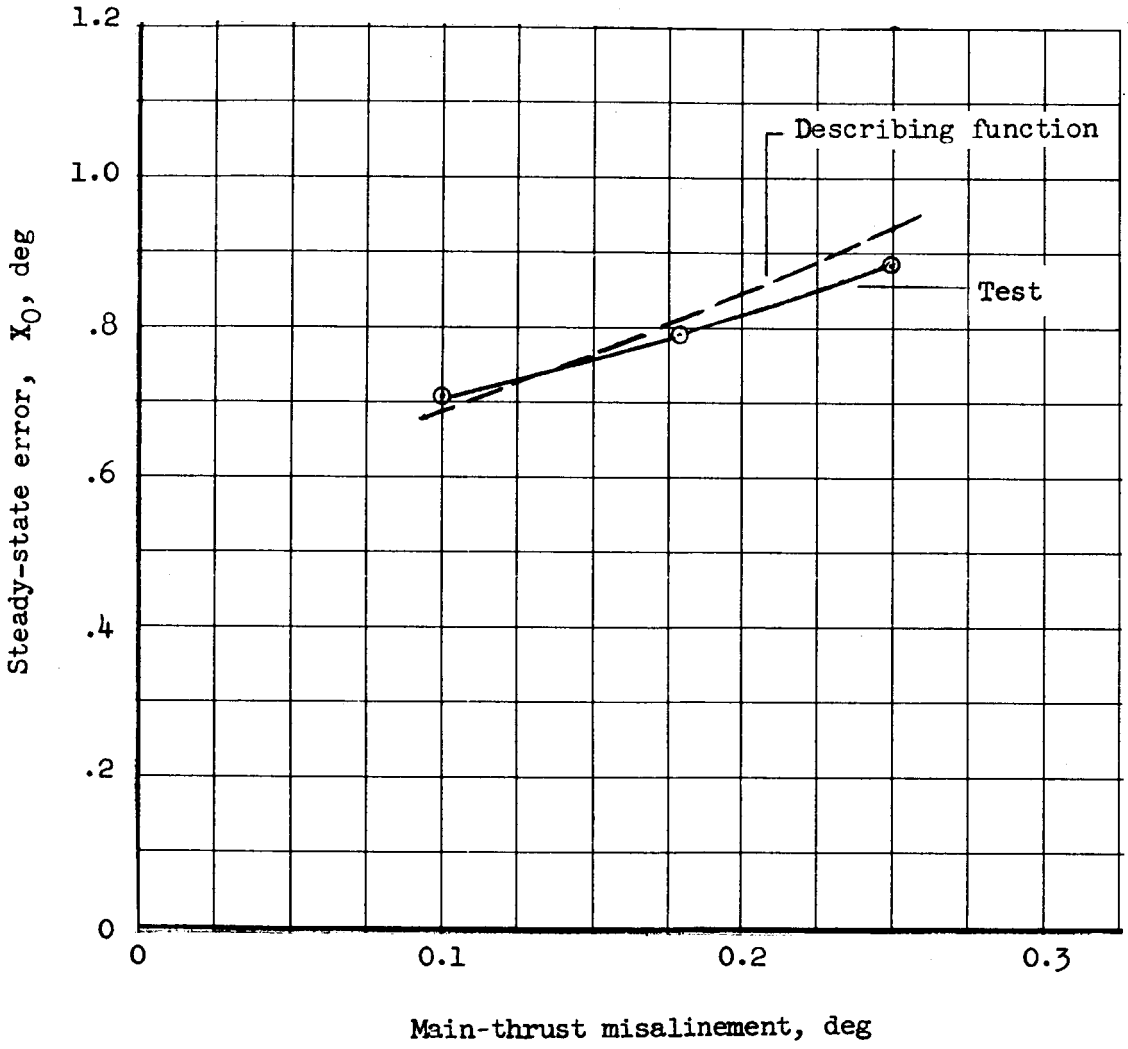

Figure 15.- Variation of steady-state error with main-thrust misalinement. (τ = 0.06 sec.)

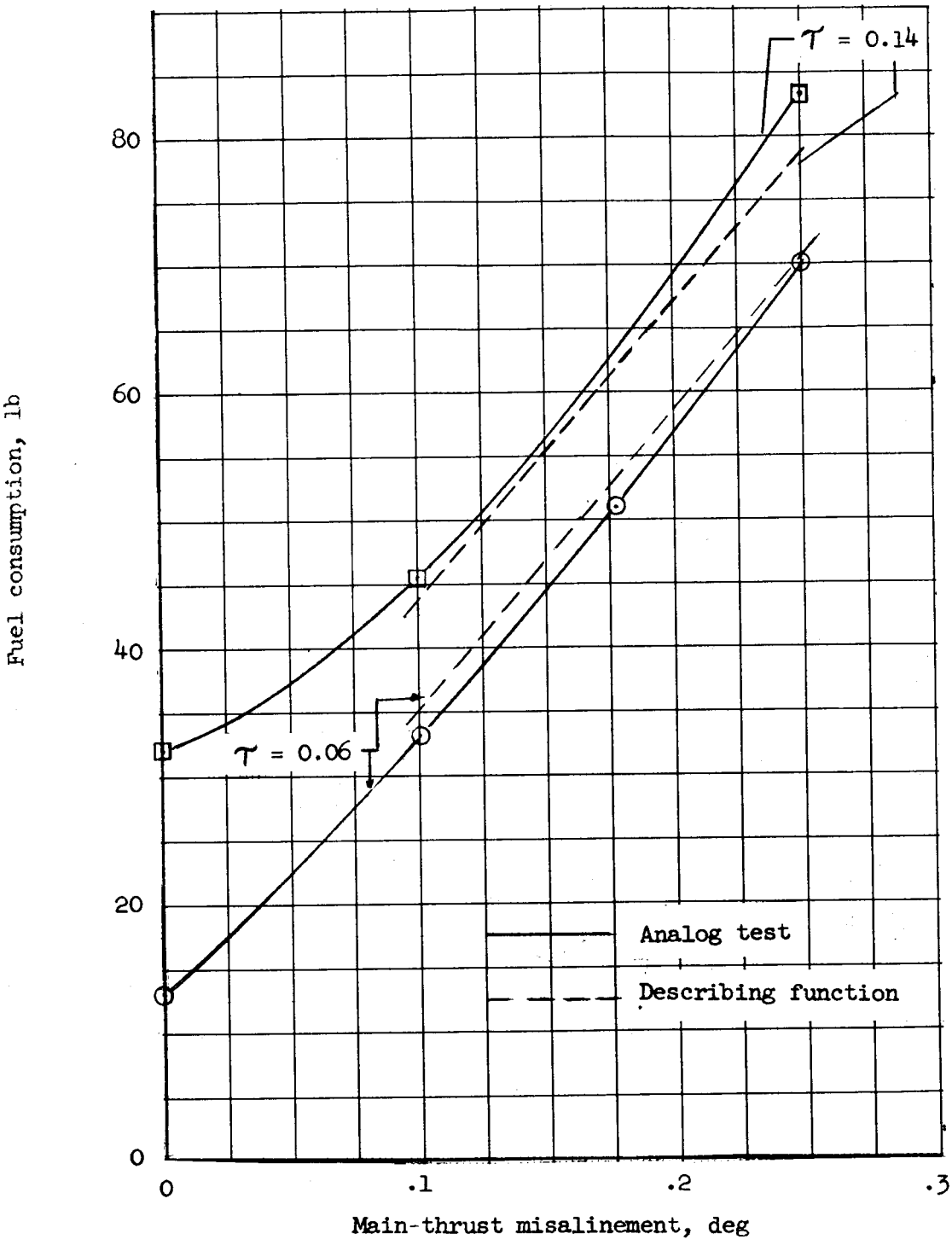

Figure 16.- Variation of fuel consumption with main-thrust misalinement. (30.85 sec burning, 5 sec coast.)

NASA - Langley Field, Va. L-1145